LncRNA LINC01871 sponging miR-142-3p to modulate ZYG11B promotes the chemoresistance of colorectal cancer cells by inducing autophagy

Bensong Duan[a]*, Haibin Zhang[a]*, Zhen Zhu[b], Xiaohan Yan[a], Zhonghua Ji[c] and Jingze Li[a]

Background **Colorectal cancer (CRC) is a malignant tumor in the digestive tract. Increasing evidence indicated that chemoresistance leads to a poor prognosis of CRC. Herein, we aimed to uncover the potential mechanism by which long intergenic noncoding RNA-1871 (LINC01871) affects the chemoresistance of CRC cells.**

Methods **Relative level of LINC01871 in CRC tissues was assessed by reverse transcription quantitative PCR (RT-qPCR). Kaplan–Meier analysis was conducted to determine the relevance of LINC01871 and the prognosis of CRC patients. Cell Counting Kit-8 (CCK-8) and colony formation assay were used to evaluate the proliferation of SW480 cells. Expression levels of proteins and their genes were assessed by western blot, immunofluorescence staining and RT-qPCR. In addition, the interaction of LINC01871, miR-142-3p and protein zyg-11 homolog B (ZYG11B) were analyzed via dual-luciferase reporter assays.**

Results **LINC01871 was low-expressed in CRC tissues and cell lines. Patients with a low level of LINC01871 showed significantly lower survival rate. pcDNA-LINC01871 significantly reduced the viability of SW480 cells ($P<0.01$), elevated SW480 cells sensitivity to 5-FU ($P<0.01$), reduced LC3 punctate aggregates ($P<0.01$) and downregulated the relative mRNA expression level of autophagy related protein 9A, autophagy related protein 4B and high mobility group box 1 ($P<0.01$) in SW480 cells. Moreover, LINC01871 was found to sponge miR-142-3p, and ZYG11B was the target of miR-142-3p. MiR-142-3p mimic significantly recovered the effect of pcDNA-LINC001871, whereas pcDNA-ZYG11B reversed the recovery effect of the miR-142-3p mimic.**

Conclusion **LINC01871/miR-142-3p/ ZYG11B axis regulates the chemoresistance of CRCs by inducing autophagy. *Anti-Cancer Drugs* 34: 827–836 Copyright © 2023 The Author(s). Published by Wolters Kluwer Health, Inc.**

Anti-Cancer Drugs 2023, **34**:827–836

Keywords: 5-FU, autophagy, chemoresistance, LINC01871, miR-142-3p, ZYG11B

[a]Department of Gastroenterology, Endoscopy Center, [b]Department of Pathology and [c]Department of Anesthesia, Shanghai East Hospital, School of Medicine, Tongji University, Shanghai, China

Correspondence to Jingze Li, MM, Department of Gastroenterology, Endoscopy Center, Shanghai East Hospital, School of Medicine, Tongji University, No. 150 Jimo Road, Shanghai 200120, China
Tel: +86 021 38804518; e-mail: dfyyxhnjkljz@163.com

*Dr. Bensong Duan and Dr. Haibin Zhang contribute equally to the writing of this article.

Received 20 August 2022 **Revised form accepted** 22 August 2022.

Introduction

Currently, colorectal cancer (CRC) is the third common malignancy in the world, with the second highest mortality rate. According to the estimated data of GLOBOCAN, an estimated 1.9 million new CRC cases and almost 0.9 million deaths occurred in 2020. The incidence and mortality of CRC are estimated to be 19.5 per 100 000, and 9.0/100 000, respectively [1]. Meanwhile, the reported number of CRC cases and CRC death cases were about 388 000 and 187 000 in China in 2015 [2]. Because CRC is a multifactorial disease, the known risk factors cause for CRC include obesity, consumption of red meat, insufficient fiber intake, alcoholism, smoking and sedentary lifestyle [3–6]. In current, chemotherapy, surgery and radiotherapy are the main treatment methods for CRC therapy. However, even though these main treatments extended the survival time of CRC patients, the prognosis is still alarming [7–9].

More and more research works have reminded the role of autophagy in CRC development [10,11]. Autophagy regulates mitochondrial function by decomposing organelles or cytoplasmic proteins under nutrient deficiency or hypoxia [12]. Meanwhile, autophagy can promote the progression of CRC [13]. And the inhibition of autophagy enhances the sensibility of CRC cells to 5-fluorouracil (5-FU) [14]. Hence, illustrating the mechanisms regulating autophagy in CRC will contribute to find new targets for CRC therapy.

Long noncoding RNAs (LncRNAs) are a kind of RNAs with exceed 200 nt in length but cannot be translated to proteins. Acting as microRNA sponges [15] or trans regulators scaffolds [16], lncRNAs play essential biological functions in CRC cell biology [17]. For example, plasma

lncRNA GAS8-AS1 is upregulated in CRC patients with early-stage, and it inhibits the proliferation of CRC cells by suppressing the lncRNA AFAP1-AS1 [18]. High expression of LncRNA TTN-AS1 was found in CRC tissues and cells, and it promotes the development of CRC by sponging miR-376a-3p and then upregulating KLF15 [19].

Increasing studies implicated LINC01871 involved in various kinds of cancers via controlling autophagy, such as cervical [20], gastric [21] and breast cancer [22]. Here, we aimed to reveal the effect of LINC01871 in the chemoresistance of CRC. Expression levels of LINC01871 and related target miRNAs and genes were measured in CRC tissues and cells. Furthermore, the potential mechanism of LINC01871 on drug susceptibility to 5-FU and autophagy were studied. This study provides novel candidates and mechanisms for the therapy of CRC.

Materials and methods

TCGA database

The expression pattern of LINC01871, miR-142-3p and ZYG11B in CRC samples were analyzed by the Encyclopedia of RNA Interactomes (ENCORI) compared with normal samples in the cancer genome atlas colon adenocarcinoma (TCGA-COAD) dataset (http://gepia.cancer-pku.cn/detail.php). Kaplan–Meier survival analysis of CRC patients was performed based on the levels of LINC01871 and miR-142-3p.

Cell culture and treatments

Four CRC cell lines SW480, HCT116, HT29 and SW620 and normal human colorectal mucosa cell line FHC (Fetal Human Colon) were obtained from the American Type Culture Collection (ATCC) of the USA. HT29 cells were cultured in Roswell Park Memorial Institute 1640, SW620, SW480 and HCT116 cells were cultured in dulbecco's modified eagle medium (DMEM), while FHC cells were cultured in DMEM/F12 added with supplements including 1% penicillin/streptomycin and 10% fetal bovine serum. The medium and the supplements were purchased from Gibco (USA). The culture condition was 37 °C with 5% CO_2. When the confluence reached 85–95%, cells were harvested for further experiments.

For chemoresistance treatment, SW480 cells were treated with 2.5, 5 or 10 μmol/L of 5-FU (Sigma-Aldrich, USA) for another 48 h.

The fragments of LINC01871 (XR_001739273.1) and ZYG11B (DQ646393.1) were cloned into pcDNA3.1 plasmid to construct LINC01871 and ZYG11B expression vectors, respectively. Mimic and inhibitor of miR-142-3p and their negative controls (NC) were synthesized by GenePharma (China). SW480 cells were transfected with pcDNA-NC, pcDNA-LINC01871 plasmids, pcDNA-ZYG11B plasmids, miR-142-3p mimic, miR-142-3p inhibitor or NC using lipofectamine 3000 (Invitrogen, USA) respectively.

Cell viability

The viability of the treated cells was evaluated according to the manual of the Cell Counting Kit-8 (CCK-8 kit) (Beyotime, China). Briefly, 0, 12, 24, 48 and 72 h after treatment, the supernatant of the treated SW48 cell was removed. Also, 100 μl of the detection reagent was injected and incubated with SW480 for another 3 h in the incubator. Then the optical density value of the treated cells was measured by a Microplate Reader (Biobase, China) at 460 nm.

Colony formation assay

This experiment was used to determine the growth of the treated cells according to the previous report [23]. Briefly, 4×10^4 of SW480 cells were inoculated in 6-well plates. Next, cells were transfected with pcDNA-NC or pcDNA-LINC01871 plasmids using lipofectamine 3000. However, 8 days later, colonies of the treated cells were stained by *2%* crystal violet for 30 min. After washing, the colonies were counted by ImageJ software (Madison, Wisconsin, USA).

StarBase analysis and dual-luciferase reporter assay

The interactions of LINC01871 and miR-142-3p, as well as ZYG11B and miR-142-3p, were predicted using StarBase (http://starbase.sysu.edu.cn/).

Dual-luciferase reporter assay was carried out as the previous description [24]. First, the full-length of the wild-type and mutant LINC01871 and ZYG11B were inserted into pmirGLO dual-luciferase vectors (Promega, USA). Then, miR-142-3p mimic or miR-NC along with wild-type/mutant reporter plasmids of LINC01871 or ZYG11B were co-transfected into SW480 cells. The relative luciferase activities were detected and calculated at about 48 h after transfection.

Reverse-transcription quantitative PCR

The total RNA of cells and tissues was extracted using Trizol (Keybio, China). Then, PrimeScript RT Kit (RR037Q; Takara, Japan) was used for reverse transcription to obtain the cDNA. The reverse transcription quantitative PCR (RT-qPCR) Kit (638314; Takara, Japan) was used for constructing the reaction system. Glyceraldehyde-3-phosphate dehydrogenase (GAPDH) and U6 were used as normalization controls. The

Table 1 The primers for reverse transcription quantitative PCR

Genes	Forward primer (5′-3′)	Reverse primer (5′-3′)
LINC01871	TCTCCCTATTCCTTACTTG	AGCCCACTGATAATGTCT
miR-142-3p [25]	GTCGTATCCAGTGCAGGG	CGACGTGTAGTGTTTCCTA
ZYG11B	GACAGATAAAGCCGTTGA	GCACTGGCAAATTCATAG
U6	CTCGCTTCGGCAGCACA	AACGCTTCACGAATTTG-CGT
GAPDH	GAACGGGAAGCTCACTGG	GCCTGCTTCACCACCT-TCT
ATG9A	GGATTGGCATCGCTAACT	GTTGAAGTGGCGGAG-GTA
ATG4B	TCAGAGCCCGTTTGGATA	CGATGAATGCGTTGAG-GAC

ATG9A, autophagy related protein 9A; ATG4B, autophagy related protein 4B; GAPDH, glyceraldehyde-3-phosphate dehydrogenase.

$2^{-\Delta\Delta Ct}$ method was applied for relative quantitative analysis of gene expression. Table 1 shows the sequences of primers, and they were synthesized by GenePharma (China).

Immunofluorescence staining

Immunofluorescence staining was performed to detect LC3 in SW480 cells in situ according to the previous description [26]. Briefly, 4×10^4 of SW480 cells were inoculated in 6-well plates and treated as required. Then, cells were fixed with the fixative for 15 min, permeabilized for 10 min, then blocked with 1% BSA for 30 min, successively. Next, LC3 primary antibody [12741S, Cell Signaling Technology (CST), USA, 50 μg/ml] was incubated overnight with the cells at 4 °C. After three washes, the cells were then incubated with a fluorescent secondary antibody (4412S, CST, 5 μg/ml) for 2 h away from light. Finally, the nucleus was stained using 4',6-diamidino-2-phenylindole (DAPI; 4083S, CST), and the images of cells were captured by the fluorescence microscope (Olympus BX51). The amount of LC3 puncta was analyzed by ImageJ.

Western blot

The treated cells were lysed with the radio immunoprecipitation assay (RIPA; Applygen, China) reagent on ice for 30 min, and then the mixture was centrifugated at 15000 g and 4 °C for 5 min to obtain the supernatant. The protein concentration was determined and compared to the standard BSA curve. After that, 20 μg of proteins were separated via 10% SDS-PAGE and then transferred to the polyvinylidine fluoride (PVDF) membrane (Absin, China). Next, the membrane was blocked with 1% skim milk for 30 min and then reacted with the required primary antibodies purchased from CST: anti-caspase-3 (14220S, 1:2000), anti-cleaved caspase-3 (9579S, 1:3000), anti-caspase-9 (20750S, 1:5000), anti-cleaved caspase-9 (20750S, 1:1000), anti-LC3 II/I (12741S, 1:5000), anti-Beclin-1 (3495S, 1:4000), anti-ULK1 (8054S, 1:3000) and anti-β-actin (4970S, 1:10000) at 4 °C overnight. On the second day, the PVDFs were rinsed with Tris-buffered saline with Tween-20 and further incubated with the secondary antibody (14708S, 1:15000) for 1 h. At last, the enhanced chemiluminescence reagent (Abbkine, USA) was used for developing, and ImageJ was used for gray analysis.

Statistical analysis

All data were obtained from at least three repeated experiments. GraphPad Prism (V6.01) was used for the statistical analysis. Student *t*-test was applied to analyze the differences between the two groups. $P<0.01$ was regarded as a statistically significant difference.

Results

LINC01871 is associated with colorectal cancer progression

To confirm the function of LINC01871 in CRC progression, the expression profiling of LINC01871 (ENSG00000235576) in CRC and normal adjacent tissues in the TCGA-COAD dataset was analyzed. The results showed that the level of LINC01871 was obviously decreased in CRC samples ($n=471$) compared to the control ($n=41$) (Fig. 1a). Additionally, patients with low-expressed LINC01871 exhibited poorer survival than those with LINC01871 (Fig. 1b). Furthermore, the expression of LINC01871 in CRC cells was remarkably lower than that in FHC cells ($P<0.01$; Fig. 1c). Because the expression level of LINC01871 in SW480 cells was the lowest, we chose SW480 cells as the model for further study.

LINC01871 inhibits proliferation of colorectal cancer cells and elevates cell sensitivity to 5-FU

To investigate the effect of LINC01871 on CRC progression, SW480 cells were transfected with pcDNA-LINC01871/NC. The introduction of

Fig. 1

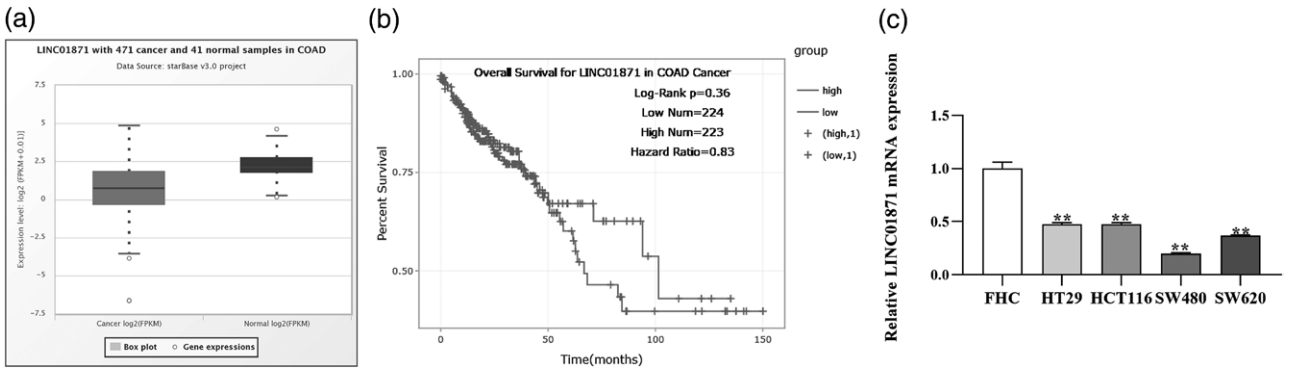

The expression level of LINC01871 was downregulated in different CRC tissues and cell lines. (a) The expression level of LINC01871 were measured by ENCORI in CRC tissues ($n = 471$) compared with normal samples ($n = 41$) from TCGA-COAD dataset (http://gepia.cancer-pku.cn/detail.php). (b) Kaplan–Meier survival analysis for CRC patients based on the expression level of lncRNA LINC01871. (c) RNA expression of LINC01871 in HT29, HCT116, SW480 and SW620 cells were measured by RT-qPCR. CRC, colorectal cancer; ENCORI, the Encyclopedia of RNA Interactomes; RT-qPCR, reverse transcription quantitative PCR; TCGA-COAD, cancer genome atlas colon adenocarcinoma.

pcDNA-LINC01871 signally reduced the viability of SW480 compared with the pcDNA-NC group ($P < 0.01$; Fig. 2a), and colony formation assay showed similar results (Fig. 2b). Furthermore, the transfected SW480 cells were treated with 2.5, 5 or 10 μmol/L of 5-FU. After 72 h of the treatment, the viability of SW480 transfected with pcDNA-LINC01871 was lower than that of pcDNA-NC-transfected cells ($P < 0.05$ with the concentration of 2.5 and 5 μmol/L; while $P < 0.001$ with the concentration of 10 μmol/L; Fig. 2c). Finally, the levels of apoptosis-related proteins in the transfected SW480 cells were tested. Both of the ratios of cleaved caspase-3 to caspase-3 and the cleaved caspase-9 to caspase-9 were reduced in the pcDNA-LINC01871 transfected cells (Fig. 2d). In combination, the above data proved that LINC01871 inhibited proliferation, promoted apoptosis of CRC cells and elevated sensibility to 5-FU.

LINC01871 inhibits autophagy of colorectal cancer cells

Then we intended to investigate the function of LINC01871 in the autophagy of CRC cells. Immunofluorescence staining, western blot and RT-qPCR were carried out to assess the expression of autophagy-related proteins. Immunofluorescence staining revealed that fewer LC3 punctate aggregates were found in pcDNA-LINC01871 transfected SW480 cells (Fig. 3a), which indicates that LINC01871 overexpression led to fewer autophagosomes. Besides, the LC3 II/I was significantly increased, whereas the expression of Beclin-1 and ULK1 was downregulated in pcDNA-LINC01871 transfected SW480 cells (Fig. 3b). In addition, the mRNA level of several ATGs including autophagy related protein 9A (ATG9A) and autophagy related protein 4B (ATG4B) were determined by RT-qPCR. All three ATGs were notably downregulated in pcDNA-LINC01871 transfected SW480 cells ($P < 0.01$; Fig. 3c). These suggested that LINC01871 inhibits the autophagy of CRC cells.

LINC01871 sponges miR-142-3p in colorectal cancer cells

Furthermore, we aimed to reveal the mechanism by which LINC01871 inhibits autophagy in CRC cells. The probable target miRNAs of LINC01871 were analyzed by bioinformatics software, and miR-142-3p was screened as the target miRNAs of LINC01871 (Fig. 4a). Dramatically, miR-142-3p mimic obviously inhibited the luciferase activity of LINC01871-WT, whereas the inhibition was abrogated in LINC01871-Mut group (Fig. 4b). Meanwhile, the transfection of miR-142-3p

Fig. 2

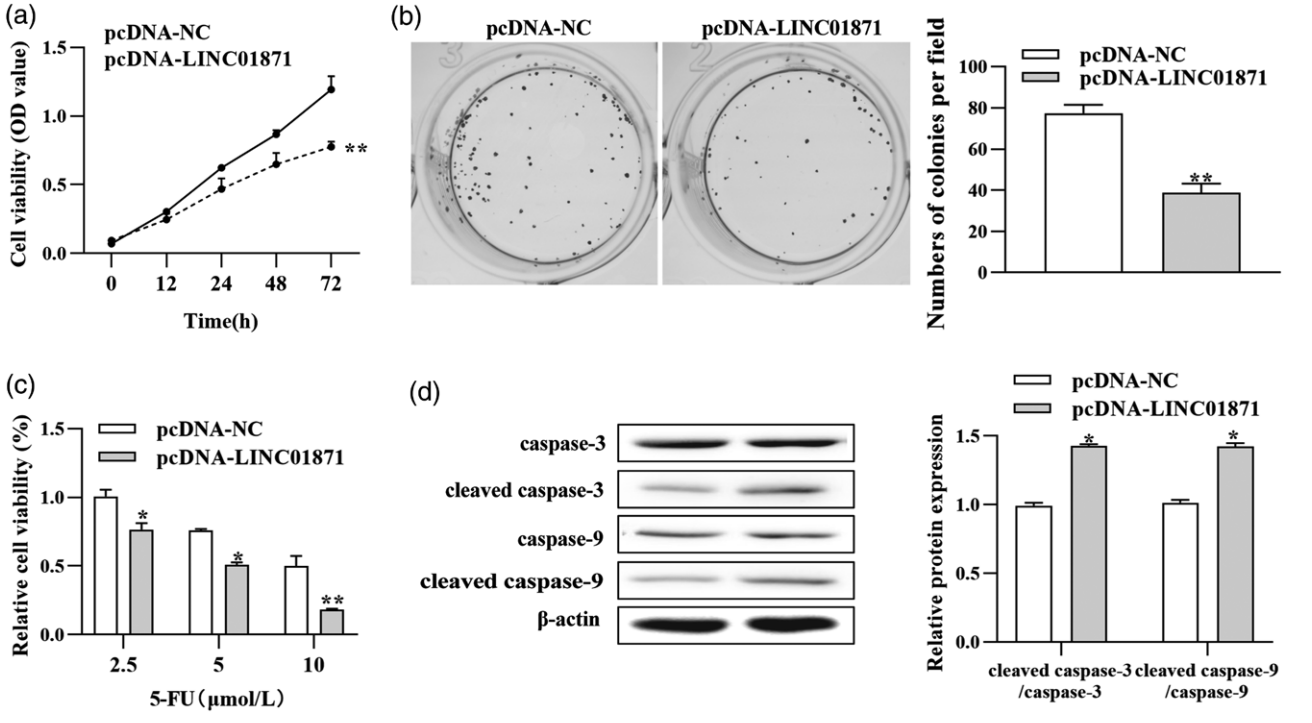

Overexpression of LINC01871 inhibited the proliferation and elevated sensitivity to 5-fluorouracil (5-FU) of SW480 cells. (a) CCK-8 results of SW480 cells when treated with pcDNA-LINC01871. (b) Colony formation results of SW480 cells when treated with pcDNA-LINC01871. (c) The sensitivity to 5-FU of SW480 cells when treated with pcDNA-LINC01871. (d) The expression level of apoptosis related proteins including caspase-3, cleaved caspase-3, caspase-9, cleaved caspase-9 in SW480 cells treated with pcDNA-LINC01871 were determined by western blotting and quantitative analysis of relative protein level. Each result was averaged from at least three independent experiments. CCK, cell counting kit-8.

Fig. 3

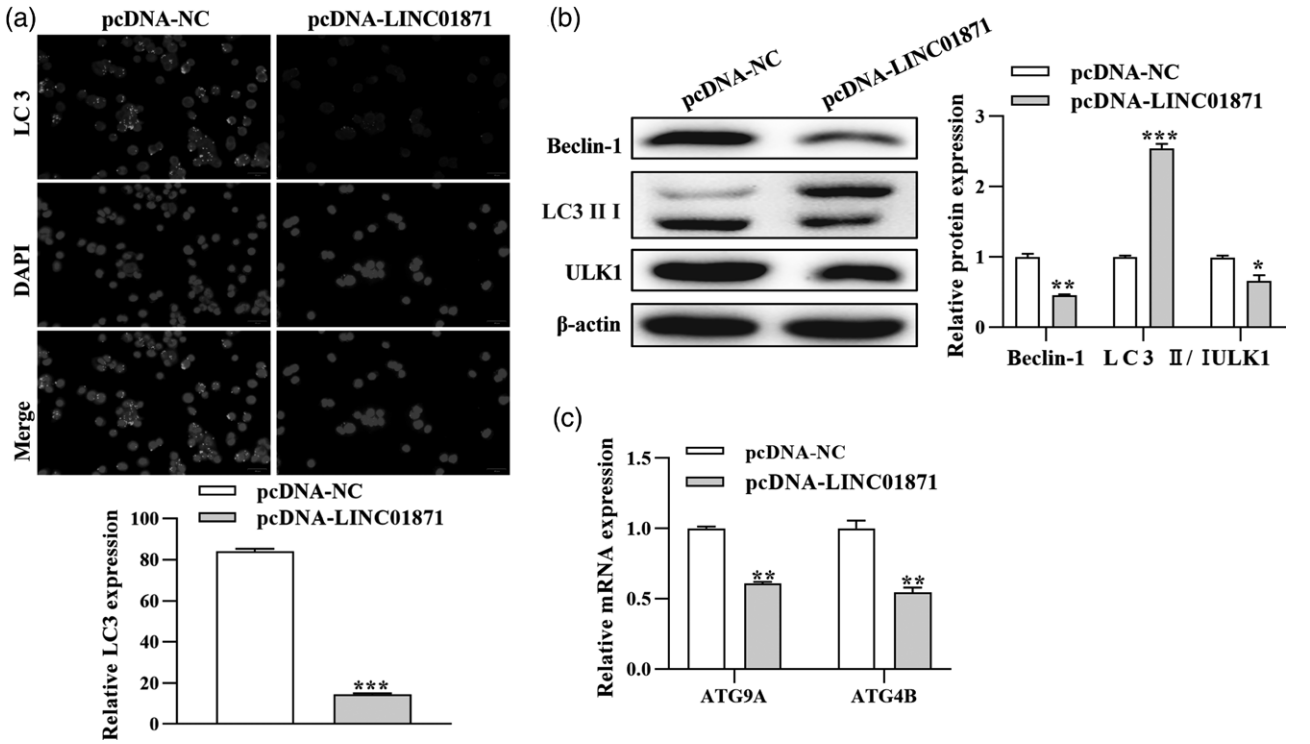

Overexpression of LINC01871 inhibited the autophagy of SW480 cells. (a) The LC3 puncta in SW480 cells treated with pcDNA-LINC01871 were determined by immunofluorescence, DAPI was used to stained nucleus and statistical comparison was performed using ImageJ software. Data are presented as the mean ± SD ($n = 3$). (b) The expression level of autophagy-related proteins including LC3 II/I, Beclin-1and ULK1 in SW480 cells treated with pcDNA-LINC01871 were determined by western blotting and quantitative analysis of relative protein level. Each result was averaged from at least three independent experiments. (c) The expression level of autophagy-related genes including ATG9A and ATG4B in SW480 cells treated with pcDNA-LINC01871 were determined by RT-qPCR. Each result was averaged from at least three independent experiments. RT-qPCR, reverse transcription quantitative PCR.

mimic reduced the level of LINC01871 in SW480 cells (Fig. 4c). The above confirmed the sponging regulation of LINC01871 to miR-142-3p.

MiR-142-3p promotes colorectal cancer progression

Next, the expression profiling of miR-142-3p (ENSG00000284353) in CRC and normal adjacent tissues was analyzed in the TCGA-COAD dataset. MiR-142-3p was dramatically upregulated in CRC samples ($n = 450$) compared with the control ($n = 8$) (Fig. 4d). Additionally, we found the high expression of miR-142-3p exhibited a positive correlation with the poor survival of patients (Fig. 4e). These results declared the acceleration of miR-142-3p to the development of CRC.

MiR-142-3p promotes the growth of colorectal cancer cells and induces chemoresistance to 5-FU

To further find out the effect of miR-142-3p level on CRC cells, we suppressed the expression of miR-142-3p in SW480 cells. The introduction of miR-142-3p inhibit signally reduced the viability of SW480 compared with NC inhibit group ($P < 0.01$; Fig. 5a). The miRNA inhibitors transfected SW480 cells were incubated with 2.5, 5 or 10 μmol/L of 5-FU. MiR-142-3p inhibitor reduced the viability of SW480 cells ($P < 0.05$ for 2.5 and 5 μmol/L 5-FU, whereas $P < 0.001$ for 10 μmol/L 5-FU; Fig. 5b).

miR-142-3p promotes the autophagy of colorectal cancer cells

The role of miR-142-3p in the autophagy of CRC cells was investigated by immunofluorescence staining, western blot and RT-qPCR. Immunofluorescence staining revealed that fewer LC3 punctate aggregates were existed in miR-142-3p-inhibited SW480 cells ($P < 0.01$; Fig. 5c), western blot showed protein expression levels of Beclin-1, ULK1 and the LC3 II/I were all downregulated in the miR-142-3p-inhibited SW480 cells ($P < 0.01$; Fig. 5d). Meanwhile, RT-qPCR exhibited that the relative mRNA level of ATG9A and ATG4B were remarkably downregulated along with the suppression of miR-142-3p ($P < 0.01$; Fig. 5e). Overall, LINC01871 inhibits the autophagy of SW480 cells via sponging miR-142-3p.

miR-142-3p downregulates ZYG11B in colorectal cancer cells

The underlying targets of miR-142-3p were analyzed by StarBase. It was predicted that ZYG11B is the target of miR-142-3p, and their binding site sequences were exhibited in

Fig. 4

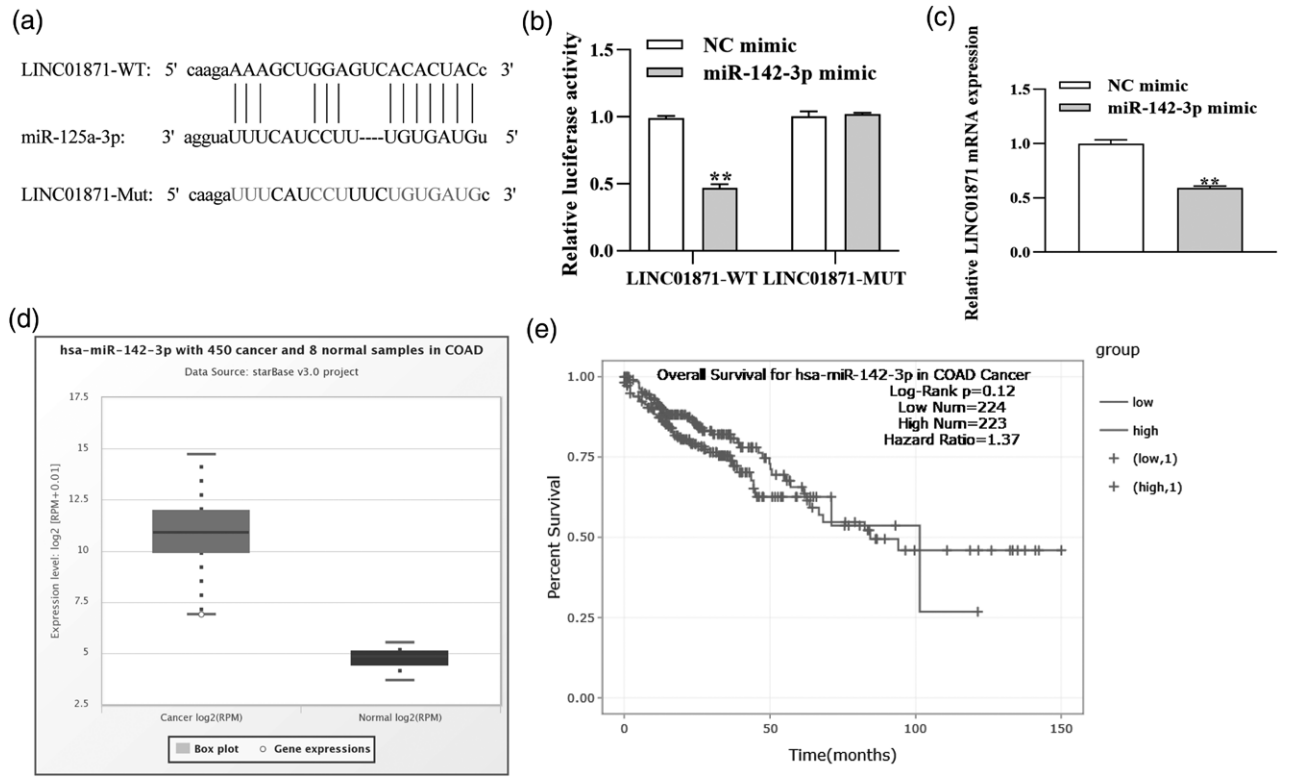

LINC01871 inhibited the autophagy of SW480 cells via sponging miR-142-3p. (a) The putative binding sites between LINC01871 and miR-142-3p were predicted by StarBase. (b) Dual-luciferase reporter assay was performed to reveal the relationship between LINC01871 and miR-142-3p. (c) The mRNA expression of LINC01871 in SW480 cells treated with miR-142-3p mimic was determined by RT-qPCR. The results were representative of three independent experiments. (d) The expression level of miR-142-3p were measured by ENCORI in CRC tissues ($n = 450$) compared with normal samples ($n = 8$) from TCGA-COAD dataset (http://gepia.cancer-pku.cn/detail.php). (e) Kaplan–Meier survival analysis for CRC patients based on the expression level of miR-142-3p. CRC, colorectal cancer; ENCORI, the Encyclopedia of RNA Interactomes; RT-qPCR, reverse transcription quantitative PCR; TCGA-COAD, cancer genome atlas colon adenocarcinoma.

Fig. 6a. Then, the targeted regulatory relationship between miR-142-3p and ZYG11B was verified. The luciferase activity of ZYG11B -WT could be inhibited by the introduction of miR-142-3p mimic, while the inhibition was abrogated in ZYG11B-MUT (Fig. 6b). Besides, the expression of ZYG11B in miR-142-3p mimic transfected SW480 cells was decreased (Fig. 6c). As a sequence, a negative relationship between ZYG11B and miR-142-3p was confirmed.

ZYG11B is associated with colorectal cancer progression

Next, the expression profiling of ZYG11B (ENSG00000162378.12) in CRC and normal adjacent tissues was analyzed in the TCGA-COAD dataset. The results showed that ZYG11B was slightly downregulated in CRC tissues ($n = 471$) compared with the control ($n = 41$) (Fig. 6d). And patients with low-expressed of ZYG11B tended to exhibit worse survival (Fig. 6e).

LINC01871 inhibits autophagy by targeting ZYG11B via sponging miR-142-3p in colorectal cancer cells

Recovery experiments were carried out to confirm the role of the LINC01871/miR-142-3p/ZYG11B axis in autophagy. As pcDNA-LINC01871 reduced the viability of SW480 cells (Fig. 7a), elevated SW480 cells' sensitivity to 5-FU (Fig. 7b), reduced LC3 punctate aggregates (Fig. 7c) and downregulated the relative mRNA expression level of ATG9A and ATG4B (Fig. 7d) in SW480 cells. MiR-142-3p mimic could markedly recover the viability (Fig. 7a), reduced sensibility to 5-FU (Fig. 7b) and attenuated autophagy activation, as the LC3 punctate aggregates were improved ($P < 0.01$; Fig. 7c) and relative mRNA expression level of ATG9A, ATG4B and high mobility group box 1 (HMGB1) were upregulated ($P < 0.01$; Fig. 7d) in SW480 cells co-transfected pcDNA-LINC01871, miR-142-3p mimic. Besides that, pcDNA-ZYG11B could reverse the recovery of the miR-142-3p mimic. As the cells viability was reduced (Fig. 7a), sensitivity to 5-FU was elevated (Fig. 7b), LC3 punctate aggregates were reduced (Fig. 7c) and the relative mRNA expression level of ATG9A and ATG4B were downregulated (Fig. 7d) in SW480 cells co-transfected pcDNA-LINC01871, miR-142-3p mimic and pcDNA-ZYG11B compared with the SW480 cells co-transfected pcDNA-LINC01871, miR-142-3p mimic and pcDNA-NC. These recovery experiments

Fig. 5.

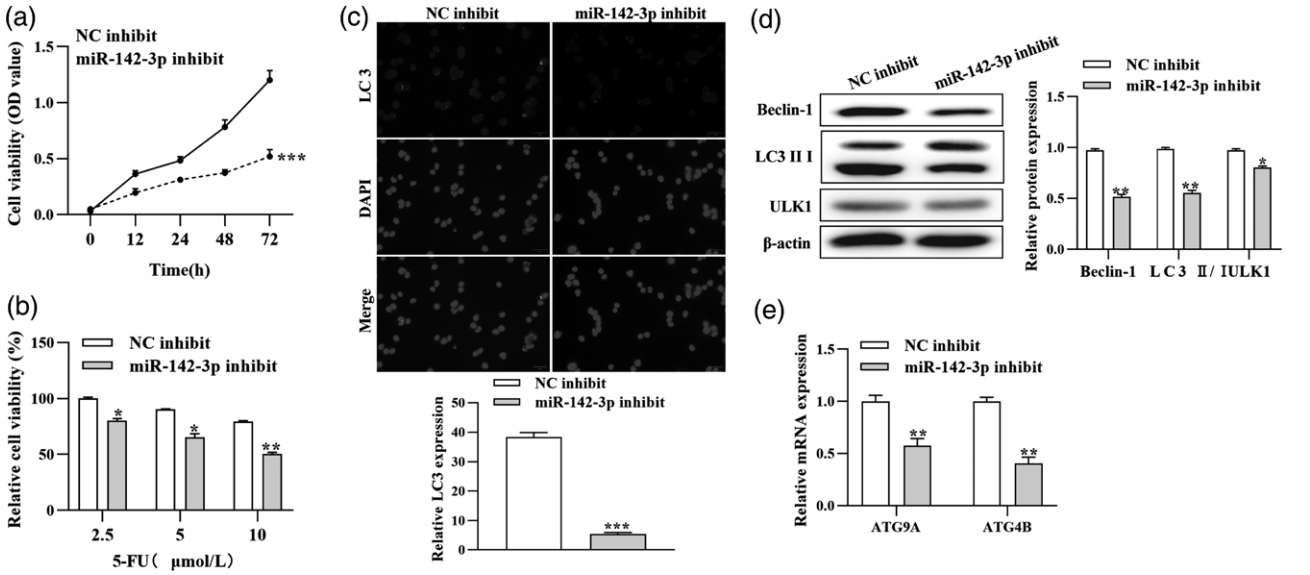

Downregulation of miR-142-3p-inhibited the autophagy of SW480 cells and reduced sensitivity to 5-fluorouracil (5-FU) of SW480 cells. (a) CCK-8 results of SW480 cells when treated with miR-142-3p inhibitor. (b) The sensitivity to 5-FU of SW480 cells when treated with miR-142-3p inhibitor. (c) The LC3 puncta in SW480 cells treated with miR-142-3p inhibitor were determined by immunofluorescence, DAPI was used to stained nucleus and statistical comparison was performed using ImageJ software. Data are presented as the mean ± SD ($n = 3$). (d) The expression level of autophagy-related proteins including LC3 II/I, Beclin-1and ULK1 in SW480 cells treated with miR-142-3p inhibitor were determined by western blotting and quantitative analysis of relative protein level. Each result was averaged from at least three independent experiments. (e) The expression level of autophagy-related genes including ATG9A and ATG4B in SW480 cells treated with miR-142-3p inhibitor were determined by RT-qPCR. Each result was averaged from at least three independent experiments. ATG9A, autophagy related protein 9A; ATG4B, autophagy related protein 4B; CCK, cell counting kit-8; RT-qPCR, reverse transcription quantitative PCR.

indeed confirmed that LINC01871 regulated autophagy of SW480 cells by targeting ZYG11B via sponging miR-142-3p.

Discussion

CRC is a serious menace to human health [1,2]. However, the therapeutic effect of the main treatments (including chemotherapy, radiotherapy and surgery) for CRC is still not ideal. A lot of evidence have suggested that CRC shows resistance to chemotherapy (such as 5-FU), which will bring poor prognosis [27]. Here, we confirmed the decreased expression of LINC01871 CRC. Overexpression of LINC01871 inhibited cell proliferation, elevated the chemosensitivity to 5-FU and promoted apoptosis in SW480 cells. This suggested that LINC01871 might be a hopeful candidate for CRC treatment.

Abnormal expression of various lncRNAs in human cancers is an essential cause of chemoresistance [28–30]. For example, Xu *et al.* [29] found patients with colon cancer with increased expression of lncRNA CASC9 suffered an unfavorable chemotherapy effect [31]. Here, we found LINC01871 was dramatically downregulated in clinical CRC samples, and patients with low-expressed LINC01871 had worse survival. Similarly, LINC01871 was low-expressed in CRC cell lines. Many studies implicated LINC01871 involved in various kinds of cancers via controlling autophagy, such as cervical [20], gastric [21] and breast cancer [22]. Wang *et al.* [32] reported that LINC01871 affects the occurrence and development of endometrial cancer by regulating autophagy. In the present study, we treated the LINC01871 overexpression SW480 cells with three different concentrations (2.5, 5 or 10 μmol/L) of 5-FU. Serious detection in LINC01871 overexpression SW480 cells showed that the relative viability of the treated cells was reduced 72 h after 5-FU treated, the ratios of cleaved caspase-3/9 to caspase-3/9 were decreased, LC3 II/I and the expression of Beclin-1and ULK1 were downregulated, the relative expression of ATG9A, ATG4B and HMGB1 in RNA level was decreased. In combination, these data confirmed that LINC01871 inhibited cell autophagy, and promoted 5-FU-induced apoptosis in SW480 cells.

Because lncRNAs play essential biological functions in CRC cell biology via sponging microRNAs [15] or scaffolding trans regulators [16]. Here, we validated that miR-142-3p was the target of LINC01871. Numerous research works have pointed out the abnormal expression of miR-142-3p in many cancers [33,34]. For instance, Chen *et al.* [33] found the upregulated miR-142-3p in carcinoma tissues and HT29 cells treated with celecoxib. In this research, the expression of miR-142-3p was verified to increase in CRC clinical samples and the high level of miR-142-3p may relate to the bad survival. In the

Fig. 6

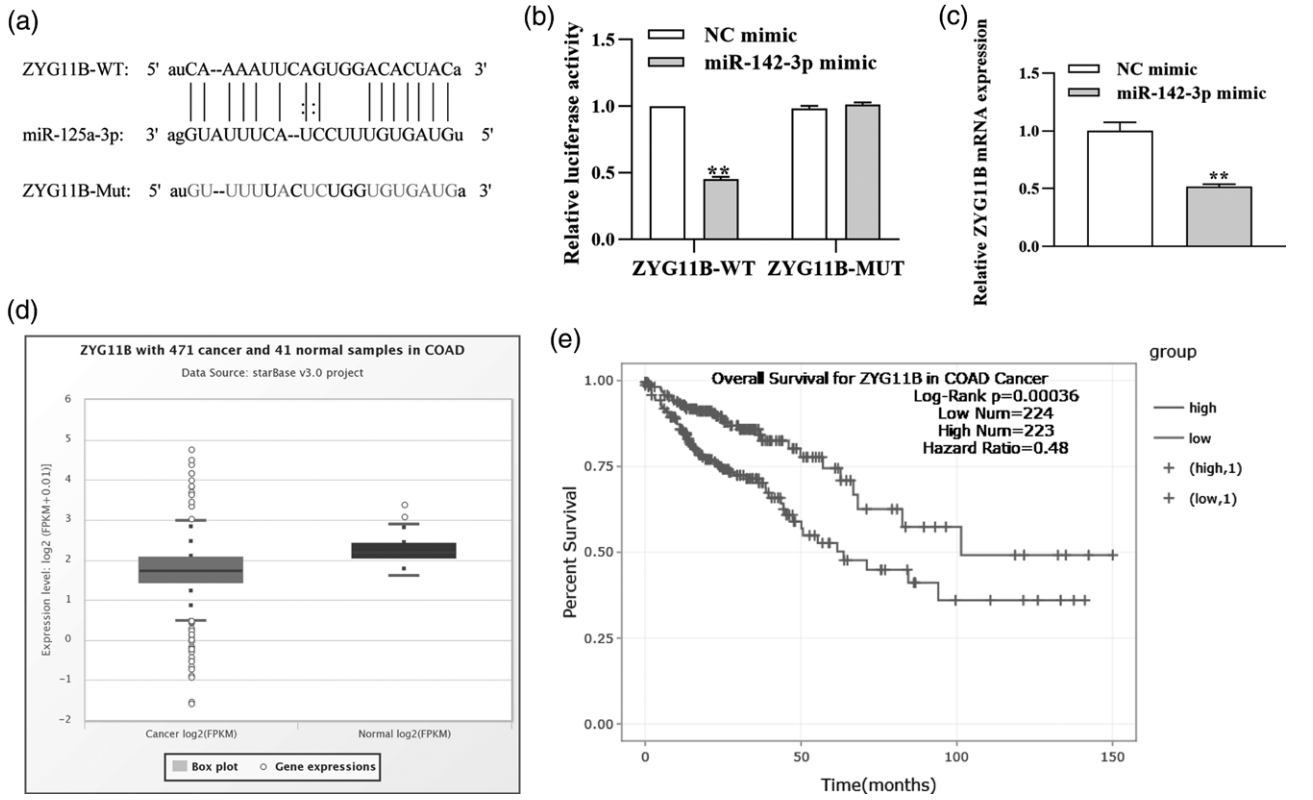

miR-142-3p targets ZYG11B. (a) The putative binding sites between ZYG11B and miR-142-3p were predicted by StarBase. (b) Dual-luciferase reporter assay was performed to reveal the relationship between ZYG11B and miR-142-3p. (c) The mRNA expression of ZYG11B in SW480 cells treated with miR-142-3p mimic was determined by RT-qPCR. The results were representative of three independent experiments. The data are presented as the mean ± SD. (d) The expression level of ZYG11B were measured by ENCORI in CRC tissues ($n = 471$) compared with normal samples ($n = 41$) from TCGA-COAD dataset (http://gepia.cancer-pku.cn/detail.php). (e) Kaplan–Meier survival analysis for CRC patients based on the expression level of ZYG11B. CRC, colorectal cancer; ENCORI, the Encyclopedia of RNA Interactomes; RT-qPCR, reverse transcription quantitative PCR; TCGA-COAD, cancer genome atlas colon adenocarcinoma.

meantime, miR-142-3p was also found upregulated in the four CRC cell lines. Yadav *et al.* [35] reported the level of miR-142-3p in the plasma of 5-FU-treated cancer-associated fibroblast-educated DLD1xenograft mouse was the highest. Here, we found the decreased expression of miR-142-3p could reduce the viability of SW480 cells, decrease the LC3 II/I and the expression of Beclin-1 and ULK1 and downregulate the relative expression of ATG9A, ATG4B and HMGB1 in RNA level. Taken together, these results suggested that LINC01871 inhibits autophagy, and promotes 5-FU-induced apoptosis via sponging miR-142-3p in CRC cells.

Through the bioinformatics prediction, we screened out ZYG11B as the direct target of miR-142-3p. ZYG11B, a subunit of the E3 ubiquitin ligase complex, is known to be involved in the clearance of proteolytic fragments produced by caspase cleavage during apoptosis [36]. Balachandran *et al.* [37] suggested that ZYG11B as the potential for antimitotic combination therapy, for ZYG11B subunit knockdown inhibited mitotic slippage in human cells. In the present study, ZYG11B overexpression could reverse the recovery of the miR-142-3p mimic. As the cells viability was reduced, sensitivity to 5-FU was elevated, LC3 punctate aggregates were reduced and the relative mRNA level of autophagy-related proteins was decreased in the SW480 cells. Besides, the decreased expression of ZYG11B was found in CRC patients, the patients with low ZYG11B expression have worse survival, and the ZYG11B expression was relatively low in the four CRC cell lines.

Conclusion

In this study, we found that LINC01871 could promote CRC cells' chemoresistance via sponging miR-142-3p to increase the level of ZYG11B. Our research may provide promising candidates for CRC therapy.

Acknowledgements

This work was supported by the Shanghai East Hospital, 'Rising Sun' Excellent Young Medical Talents Training Program (NO. 2019xrrcjh01).

The datasets used and analyzed during the current study are available from the corresponding author on reasonable request.

Fig. 7

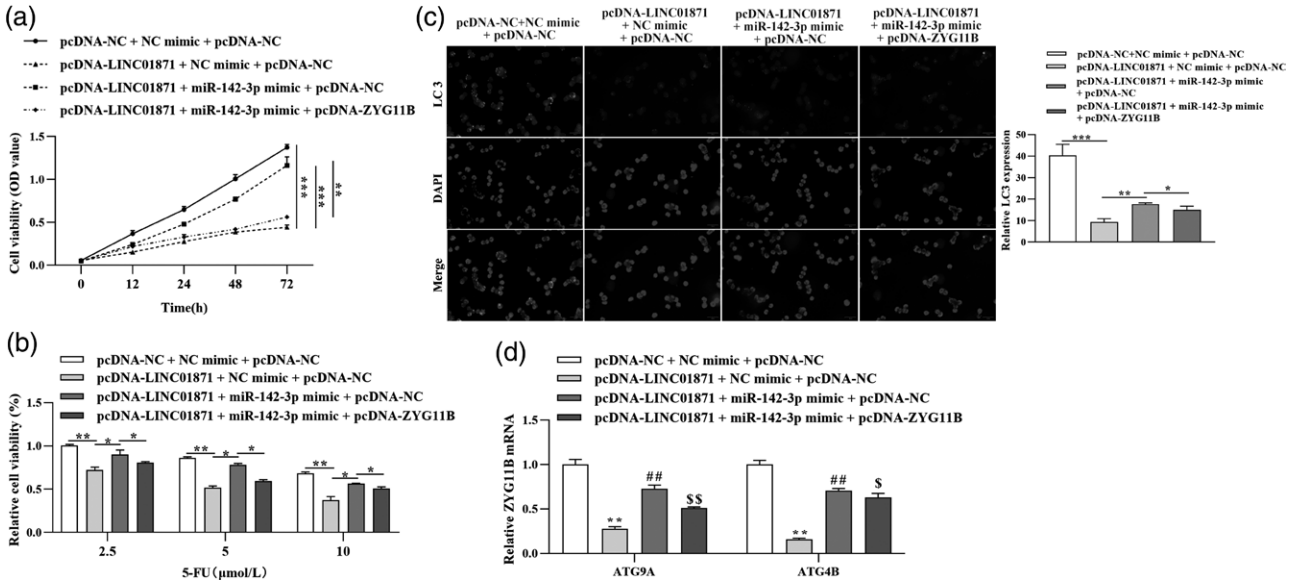

Overexpression of ZYG11B reversed the effect of miR-142-3p upregulation on SW480 cells. pcDNA-LINC01871 or pcDNA-NC and miR-142-3p mimic or NC mimic along with pcDNA-ZYG11B were co-transfected into SW480 cells. After transfection, the cells were seeded into appropriate cell culture plates for further assay. (a) Cell proliferation of the treated SW480 cells were measure by CCK-8. (b) Cell viability of the treated SW480 cells were measure by CCK-8. (c) The LC3 puncta in the treated SW480 cells were determined by immunofluorescence, DAPI was used to stained nucleus and statistical comparison was performed using ImageJ software. Data are presented as the mean ± SD ($n = 3$). (d) The expression level of autophagy-related genes including ATG9A and ATG4B in the treated SW480 cells were determined by RT-qPCR. Each result was averaged from at least three independent experiments. ATG9A, autophagy related protein 9A; ATG4B, autophagy related protein 4B; CCK, cell counting kit-8; RT-qPCR, reverse transcription quantitative PCR.

Z.J. and J.L. designed the study. B.D. and H.Z. performed the experiment and drafted the manuscript. Z.Z. performed the literature search and data analysis. X.Y. contributed to the data analysis. B.D. and H.Z. discussed the results. Z.Z. and X.Y. contributed to cell culture. Z.J., J.L., B.D. and H.Z. revised the article. All authors reviewed the article.

Conflicts of interest

There are no conflicts of interest.

References

1 Sung H, Ferlay J, Siegel RL, Laversanne M, Soerjomataram I, Jemal A, *et al.* Global Cancer Statistics 2020: GLOBOCAN estimates of incidence and mortality worldwide for 36 cancers in 185 countries. *CA Cancer J Clin* 2021; **71**:209–249.

2 Zheng RS, Sun KX, Zhang SW, Zeng HM, Zou XN, Chen R, *et al.* [Report of cancer epidemiology in China, 2015]. *Zhonghua Zhong Liu Za Zhi* 2019; **41**:19–28.

3 Loke YL, Chew MT, Ngeow YF, Lim WWD, Peh SC. Colon carcinogenesis: the interplay between diet and gut microbiota. *Front Cell Infect Microbiol* 2020; **10**:603086.

4 Pathak S, Pandanaboyana S, Daniels I, Smart N, Prasad KR. Obesity and colorectal liver metastases: mechanisms and management. *Surg Oncol* 2016; **25**:246–251.

5 Perše M. Oxidative stress in the pathogenesis of colorectal cancer: cause or consequence? *Biomed Res Int* 2013; **2013**:725710.

6 Davidson NO. Genetic testing in colorectal cancer: who, when, how and why. *Keio J Med* 2007; **56**:14–20.

7 Morkavuk SB, Güner M, Tez M, Ünal AE. The outcomes of isolated ureteral resection and reconstruction in non-urologic cancer patients who underwent cytoreductive surgery (CRC) and hyperthermic intraperitoneal chemotherapy (HIPEC). *World J Surg Oncol* 2019; **17**:230.

8 Houghton J, Baum M, Haybittle JL. Role of radiotherapy following total mastectomy in patients with early breast cancer. The closed trials working party of the CRC breast cancer trials group. *World J Surg* 1994; **18**:117–122.

9 Tannapfel A, Reinacher-Schick A. Chemotherapie-assoziierte Hepatotoxizität in der Behandlung des kolorektalen Karzinoms (KRK) [Chemotherapy associated hepatotoxicity in the treatment of advanced colorectal cancer (CRC)]. *Z Gastroenterol* 2008; **46**:435–440.

10 Auger C, Christou N, Brunel A, Perraud A, Verdier M. Autophagy and extracellular vesicles in colorectal cancer: interactions and common actors? *Cancers (Basel)* 2021; **13**:1039.

11 He Q, Li Z, Yin J, Li Y, Yin Y, Lei X, *et al.* Prognostic significance of autophagy-relevant gene markers in colorectal cancer. *Front Oncol* 2021; **11**:566539.

12 Breininger SP, Malcomson FC, Afshar S, Turnbull DM, Greaves L, Mathers JC. Effects of obesity and weight loss on mitochondrial structure and function and implications for colorectal cancer risk. *Proc Nutr Soc* 2019; **78**:426–437.

13 Huang G, Liu Z, He L, Luk KH, Cheung ST, Wong KH, *et al.* Autophagy is an important action mode for functionalized selenium nanoparticles to exhibit anti-colorectal cancer activity. *Biomater Sci* 2018; **6**:2508–2517.

14 Liu MP, Liao M, Dai C, Chen JF, Yang CJ, Liu M, *et al.* Sanguisorba officinalis L synergistically enhanced 5-fluorouracil cytotoxicity in colorectal cancer cells by promoting a reactive oxygen species-mediated, mitochondria-caspase-dependent apoptotic pathway. *Sci Rep* 2016; **6**:34245.

15 Liu D, Li Y, Luo G, Xiao X, Tao D, Wu X, *et al.* LncRNA SPRY4-IT1 sponges miR-101-3p to promote proliferation and metastasis of bladder cancer cells through up-regulating EZH2. *Cancer Lett* 2017; **388**:281–291.

16 Andric V, Nevers A, Hazra D, Auxilien S, Menant A, Graille M, *et al.* A scaffold lncRNA shapes the mitosis to meiosis switch. *Nat Commun* 2021; **12**:770.

17 Ma ML, Zhang HY, Zhang SY, Yi XL. LncRNA CDKN2B-AS1 sponges miR-28-5p to regulate proliferation and inhibit apoptosis in colorectal cancer. *Oncol Rep* 2021; **46**:213.

18 Zhao Y, Chu Y, Sun J, Song R, Li Y, Xu F. LncRNA GAS8-AS inhibits colorectal cancer (CRC) cell proliferation by downregulating lncRNA AFAP1-AS1. *Gene* 2019; **710**:140–144.

19 Yao Y, Wang X, Gao J. LncRNA KCNQ1OT1 sponges miR-206 to ameliorate neural injury induced by anesthesia via up-regulating BDNF. *Drug Des Devel Ther* 2020; **14**:4789–4800.
20 Chen Q, Hu L, Huang D, Chen K, Qiu X, Qiu B. Six-lncRNA immune prognostic signature for cervical cancer. *Front Genet* 2020; **11**:533628.
21 He Y, Wang X. Identification of molecular features correlating with tumor immunity in gastric cancer by multi-omics data analysis. *Ann Transl Med* 2020; **8**:1050.
22 Li X, Li Y, Yu X, Jin F. Identification and validation of stemness-related lncRNA prognostic signature for breast cancer. *J Transl Med* 2020; **18**:331.
23 Gholamzadeh Khoei S, Saidijam M, Amini R, Jalali A, Najafi R. Impact of PIN1 inhibition on tumor progression and chemotherapy sensitivity in colorectal cancer. *J Gastrointest Cancer* 2022; **53**:299–310.
24 Liu F, Ai FY, Zhang DC, Tian L, Yang ZY, Liu SJ. LncRNA NEAT1 knockdown attenuates autophagy to elevate 5-FU sensitivity in colorectal cancer via targeting miR-34a. *Cancer Med* 2020; **9**:1079–1091.
25 Lei Z, Xu G, Wang L, Yang H, Liu X, Zhao J, *et al*. MiR-142-3p represses TGF-β-induced growth inhibition through repression of TGFβR1 in non-small cell lung cancer. *FASEB J* 2014; **28**:2696–2704.
26 Qin Y, Sun W, Zhang H, Zhang P, Wang Z, Dong W, *et al*. LncRNA GAS8-AS1 inhibits cell proliferation through ATG5-mediated autophagy in papillary thyroid cancer. *Endocrine* 2018; **59**:555–564.
27 Blondy S, David V, Verdier M, Mathonnet M, Perraud A, Christou N. 5-Fluorouracil resistance mechanisms in colorectal cancer: from classical pathways to promising processes. *Cancer Sci* 2020; **111**:3142–3154.
28 Kresoja-Rakic J, Szpechcinski A, Kirschner MB, Ronner M, Minatel B, Martinez VD, *et al*. miR-625-3p and lncRNA GAS5 in liquid biopsies for predicting the outcome of malignant pleural mesothelioma patients treated with neo-adjuvant chemotherapy and surgery. *Noncoding RNA* 2019; **5**:41.
29 Xu YH, Tu JR, Zhao TT, Xie SG, Tang SB. [Corrigendum] Overexpression of lncRNA EGFR-AS1 is associated with a poor prognosis and promotes chemotherapy resistance in non-small cell lung cancer. *Int J Oncol* 2019; **55**:340.
30 Gong WJ, Yin JY, Li XP, Fang C, Xiao D, Zhang W, *et al*. Association of well-characterized lung cancer lncRNA polymorphisms with lung cancer susceptibility and platinum-based chemotherapy response. *Tumour Biol* 2016; **37**:8349–8358.
31 Jiao Y, Liu Q, Zhao H, Hu X, Sun J, Liu X. Changes and prognostic value of lncRNA CASC9 in patients with advanced colon cancer after chemotherapy. *Evid Based Complement Alternat Med* 2021; **2021**:1858974.
32 Wang Z, Zhang J, Liu Y, Zhao R, Zhou X, Wang H. An integrated autophagy-related long noncoding RNA signature as a prognostic biomarker for human endometrial cancer: a bioinformatics-based approach. *Biomed Res Int* 2020; **2020**:5717498.
33 Chen WC, Lin MS, Ye YL, Gao HJ, Song ZY, Shen XY. microRNA expression pattern and its alteration following celecoxib intervention in human colorectal cancer. *Exp Ther Med* 2012; **3**:1039–1048.
34 Shang A, Gu C, Wang W, Wang X, Sun J, Zeng B, *et al*. Exosomal circPACRGL promotes progression of colorectal cancer via the miR-142-3p/miR-506-3p- TGF-β1 axis. *Mol Cancer* 2020; **19**:117.
35 Yadav VK, Huang YJ, George TA, Wei PL, Sumitra MR, Ho CL, *et al*. Preclinical evaluation of the novel small-molecule MSI-N1014 for treating drug-resistant colon cancer via the LGR5/β-catenin/miR-142-3p network and reducing cancer-associated fibroblast transformation. *Cancers (Basel)* 2020; **12**:1590.
36 Yamaki Y, Kagawa H, Hatta T, Natsume T, Kawahara H. The C-terminal cytoplasmic tail of hedgehog receptor patched1 is a platform for E3 ubiquitin ligase complexes. *Mol Cell Biochem* 2016; **414**:1–12.
37 Balachandran RS, Heighington CS, Starostina NG, Anderson JW, Owen DL, Vasudevan S, *et al*. The ubiquitin ligase CRL2ZYG11 targets cyclin B1 for degradation in a conserved pathway that facilitates mitotic slippage. *J Cell Biol* 2016; **215**:151–166.